



HAL
open science

Biological Applications and Toxicity Minimization of Semiconductor Quantum Dots

Samira Filali, Fabrice Pirot, Pierre Miossec

► **To cite this version:**

Samira Filali, Fabrice Pirot, Pierre Miossec. Biological Applications and Toxicity Minimization of Semiconductor Quantum Dots. Trends in Biotechnology, 2020, 38, pp.163 - 177. 10.1016/j.tibtech.2019.07.013 . hal-03489685

HAL Id: hal-03489685

<https://hal.science/hal-03489685>

Submitted on 21 Jul 2022

HAL is a multi-disciplinary open access archive for the deposit and dissemination of scientific research documents, whether they are published or not. The documents may come from teaching and research institutions in France or abroad, or from public or private research centers.

L'archive ouverte pluridisciplinaire **HAL**, est destinée au dépôt et à la diffusion de documents scientifiques de niveau recherche, publiés ou non, émanant des établissements d'enseignement et de recherche français ou étrangers, des laboratoires publics ou privés.



Distributed under a Creative Commons Attribution - NonCommercial 4.0 International License

1
2
3
4
5
6
7
8
9
10
11
12
13
14

Review

Biological applications and toxicity minimization of semiconductor quantum dots

Samira Filali^{a,b}, Fabrice Pirot^b, Pierre Miossec^{a*}

^a Immunogenomics and Inflammation Research Unit EA 4130, Department of Immunology and Rheumatology, Edouard Herriot Hospital, Hospices Civils de Lyon, University of Lyon, Lyon, France

^b Laboratory of Research and Development of Industrial Galenic Pharmacy and laboratory of Tissue Biology and Therapeutic Engineering UMR-CNRS 5305, Pharmacy Department, FRIPHARM Plateform, Edouard Herriot Hospital, Hospices Civils de Lyon, University of Lyon, Lyon, France, Fripharm.com

*Correspondence: samira.filali@chu-lyon.fr (Dr. Samira FILALI)

Keywords: quantum dots, stem cells, differentiated cells, organs, animal species

15 **Abstract**

16 The extraordinary potential of semiconductor quantum dots (QDs) has resulted in their
17 widespread application in various fields, from engineering technology and development of
18 laboratory techniques to biomedical imaging and therapeutic strategies. However, the toxicity
19 of QDs remains a concern and has limited their applications in human health. Better
20 understanding the behavior of QDs as it relates to their composition will enable exploring their
21 limitations and developing a strategy to control their toxicity for potential therapeutic
22 applications. Here, approaches to minimize their toxicities according to the specific cell type,
23 organ, or animal species are described. This review summarizes recent promising works at the
24 levels of cells, organs, and whole organisms.

25

26

27 **Potential of QDs in the biological fields**

28 The multitude of researchers exploring the remarkable potential of **quantum dots** (QDs) (see
29 Glossary, Box 1 and 2) in biomedical research, from tools in medical imaging to the
30 development of sophisticated theranostic agents, indicate the great potential of QDs in this field.
31 Among the variety of nanoprobe (upconversion nanoparticles, fluorescent proteins, and
32 graphene-based nanomaterials), semiconductor QDs have distinguished themselves in the field
33 of imaging due to their size and their optical properties (stable fluorescence, brightness) and
34 cost-effectiveness relative to conventional fluorescent dyes. Their extremely small size (order
35 of magnitude of biological molecules, 1 -10 nm) makes these QDs ideal candidates for
36 identification and tracking of biomolecules and organelles inside the cell and especially in the
37 nucleus, unlike upconversion nanoparticles that have a larger size (20-50 nm) and cannot reach
38 the nucleus[1]. Moreover, unlike carbon dots, red fluorescence emission for QDs
39 semiconductors, which is the preferred color in biological applications due to cells
40 autofluorescence phenomena in the 400 to 600 nm range (yellow, green, blue), is possible with
41 semiconductor QDs. As a result, despite the toxicity conferred by semiconductor QDs (although
42 recently controversial for so-called "biocompatible" nanoparticles), better understanding the
43 occurrence of their toxicity and strategies to minimize their toxicity would enable their better
44 use. In targeted imaging, QDs targeting tumors or biomarkers play a crucial role in the
45 detection, treatment, monitoring, and prognostic evaluation of certain diseases. However, for
46 purely diagnostic applications, in which cell damage must be avoided, the potential toxicity
47 caused by the release of metal ions remains a major limitation to the use of QDs, thereby
48 hindering their translation from preclinical studies to clinical studies in biomedical imaging. A
49 number of reviews have been published to address various questions, including the recent
50 progress made on QD surface modification, describing their structure-activity relationships
51 (Figure 1), mechanisms of uptake in cells, and biomedical applications. However, few reviews

52 have specifically presented a body of knowledge that enables a detailed overview on the
53 behavior of QDs including or not means to minimize toxicity according to the specific cell type,
54 tissue/organ, or animal species. This review aims to collate information on recent advances in
55 the use of QDs in biological fields, with the objective of describing the various effects of QDs
56 reported thus far, and to elucidate their behavior in living organisms, notably for future
57 applications in humans.

58

59 **Application of QDs at the cellular level**

60 **Stem cells** (see Glossary) are able to multiply indefinitely *in vitro* in an undifferentiated state,
61 and can differentiate in the presence of adequate factors. QDs have proved to be of great value
62 in cell imaging, particularly in the monitoring of cell differentiation, and in functional studies.
63 However, the biological effect may differ depending on the type of stem cell or differentiated
64 cell (Table 1).

65

66 *Stem cells*

67 The hemocompatibility of QDs was assessed in hematopoietic stem cells by combining Tat
68 Peptide with CdSe/ZnS-QDs, which made it possible to monitor transplantation successfully
69 [2]. However, in differentiated hematopoietic cells (human blood neutrophil granulocytes,
70 monocytes, lymphocytes, and platelets), harmful effects were observed that were specific to
71 both their morphology (maximum accumulation of QDs with monocytes and minimum with
72 lymphocytes) and function (despite the presence of the shell, neutrophils underwent cell death
73 after phagocytosis of CdSe/ZnS-QDs, and CdTe-QD-induced platelet aggregation in the
74 absence of plasma) [3,4].

75 Concerning epithelial stem cells, depending on QD composition, the effects may be either
76 deleterious or beneficial. Several studies have provided explanations for the cytotoxic effects

77 of QDs, which occur notably via interaction of CdTe-QDs with aromatic rings and amine
78 groups from trans-membrane proteins and the cytoskeleton[5], and the predomination of the
79 overall cellular response, which is mediated by the minor non-endocytic uptake of CdSe/ZnS-
80 QDs in BEAS-2B human bronchial epithelial cells [6]. Despite the use of multi-shell CdSe-
81 CdS/ZnS-QDs in the Calu-3 human lung cell monolayer, mechanical stress and activation of
82 Ca^{2+} influx were induced, affecting the lung barrier [7]. However, a different study showed that
83 these QDs did not elicit noticeable changes in the long-term **TEER** (see Glossary) after a
84 70 day-exposure, suggesting their potential use for drug delivery at the surface of the lung
85 epithelium for short periods [8]. Glass incorporation in CdSe-QDs in place of coating by greater
86 polymer-enabled reduction of the cytotoxicity on HaCaT keratinocytes. The higher rigidity and
87 density of glass relative to polymer enabled more efficient blocking of Cd and Se ions, making
88 these QDs safer for biological applications [9].

89 Nerve stem cells (NSCs) appear to be more resistant than other stem cells. After uptake, mainly
90 via microfilaments and microtubules, CdSe/ZnS-polymer-QDs and graphene-QDs had little
91 effect on the growth and proliferation of primary NSCs within a week[10,11]. CdSe/ZnS-QDs
92 did not affect either differentiation potential of NSCs or the protein expression of neuron- and
93 astrocyte-derived primary nerve stem cells [11]. In the GT1-7 differentiated neuronal cell line,
94 CdSe/ZnS-QDs were incorporated into only a limited fraction of the whole lysosomal
95 compartment, inducing a slight but significant reduction in cell survival and proliferation [12].

96 Mesenchymal stem cells are important for synthesizing and repairing the musculoskeletal
97 system (such as cartilage cells, bone cells, fat cells, synovial cells, or myoblasts). QDs have
98 been mainly used for the characterization of these cell types, with a majority of the QDs having
99 no negative impact on cell viability and differentiation [13,14]. The use of ZnS/CdSe-
100 streptavidin-QDs conjugated with a Fab fragment of an anti-myc antibody enabled the tracking
101 of GLUT4 movement in 3T3L1 adipocytes after stimulation by insulin or in an insulin-resistant

102 state [15]. The composition of CdSe/ZnS-polymer-QDs conjugated with a unique antibody
103 against a heat shock chaperone (mortalin) allowed the successful tracking of mesenchymal stem
104 cells labeled during tissue repair, following 26 weeks of allogeneic transplantation in a rabbit
105 model of osteochondral defects [16]. The construction of a siRNA-coupled CdSe/ZnS-PEG-
106 QDs has been successfully achieved, and has both demonstrated the involvement of *SOX9* in
107 chondrogenesis and enabled the real-time monitoring of transfection [17]. CdTe-QDs have
108 allowed the simultaneous characterization of two types of cadmium-induced cell death
109 (apoptosis and autophagy) [18].

110 QD toxicity in male and female germ cells and during embryonic development has also been
111 evaluated. At concentrations between 1 and 125 nM of CdSe-QDs, no toxicity was detected in
112 germ cells (i.e., in terms of viability and motility of spermatozoa) and embryos. At 500 nM,
113 toxic effects on both pre-and post-implantation embryo development and female germ cells
114 (with decreased maturation and fertilization rates) were reported, which were reduced with the
115 incorporation of a ZnS shell. The transfer across the placental barrier resulted in Cd
116 accumulation in pups, which was reduced after coating with PEG or SiO₂ [19].

117

118 *Differentiated cells*

119 Overall, Cd²⁺-based QDs had deleterious effects in hepatic cells, including CdSe/ZnS-QDs-
120 induced L02 hepatocyte pyroptosis, liver inflammation, and dysfunction[20], as well as CdTe-
121 QD-induced mitochondrial damage in human hepatocellular carcinoma cells (HepG2), which
122 were not solely attributable to cadmium released from QDs, as the observed effects were similar
123 or greater to those of cadmium chloride[21]. However, graphene-QDs did not induce
124 cytotoxicity in mouse primary hepatocytes [22].

125 An extensive investigation of the signaling mechanism involved in the induction of cytotoxicity
126 of shell-less QDs has been performed in endothelial cells; notably, the pathways implicated in

127 CdTe-QDs-mediated mitochondrial-dependent apoptosis in human umbilical vein endothelial
128 cells have been studied in detail [23]. Nevertheless, the use of shells or an amorphous form [24]
129 seems sufficient to reduce their toxicity. Furthermore, additional applications may emerge
130 following the discovery of stronger accumulation of CdSe/ZnS-QDs in slow-flowing, small
131 caliber venous vessels than in fast-flowing, high caliber arterial vessels [25] and the large-scale
132 internalization of CdSe/ZnS-QDs conjugated to monoclonal antibodies targeting the murine
133 transferrin receptor (Ri7) by brain capillary endothelial cells [26].

134 The effects of unshelled QDs in nephrocytes have been discussed in detail. L-cysteine-capped
135 CdTe-QDs decreased cell viability and modified the structure and activity of copper-zinc
136 superoxide dismutase in mouse primary nephrocytes and hepatocytes. Notably, this effect was
137 abrogated by the addition of ascorbic acid [27]. The study of pig renal cells revealed the
138 involvement of the Wnt pathway in CdTe-QDs-induced damage [27]. The evaluation of the
139 nephrotoxicity in HK-2 human epithelial tubular cells using various metallic QDs with
140 differential solubility (TiO₂, ZnO, and CdS) revealed that soluble CdS- and ZnO-QDs elicited
141 cell death in a dose-dependent manner, and this effect was attributed to the release of metallic
142 cations. However, insoluble TiO₂-QDs had no cytotoxic effect [28]. Targeting bladder
143 urothelial cancer cells was performed successfully using CdSe/ZnS-QDs conjugated with the
144 prostate stem cell antigen [29].

145 Recently, promising applications in both diagnostics and therapy of microbial infections have
146 been reported. QD-specific antibodies designed for use as biosensors via the association of
147 rabbit anti-p38 antibody and CdSe/ZnS-QDs, were shown to successfully infiltrate porous
148 silicon whose pores contained immobilized Egp38 antigen. These QDs were used to detect
149 *Echinococcus granulosus* for early diagnosis of hydatid disease [30]. Photoexcited QDs have
150 been used to kill a wide range of multidrug-resistant bacterial clinical isolates, including
151 methicillin-resistant *Staphylococcus aureus*, carbapenem-resistant *Escherichia coli*, extended-

152 spectrum β -lactamase-producing *Klebsiella pneumoniae*, and *Salmonella typhimurium*, while
153 leaving mammalian cells intact. Their proposed application in clinical phototherapy is
154 suggested for the treatment of infections [31].

155

156 **Application of QDs in organs**

157 *Ex vivo* investigation would enable elucidation of QD-induced effects on a collection of
158 specific cells in their environment. The different applications of QDs were grouped by organ
159 system in this review (Table 2).

160

161 *Integumentary system*

162 Several studies have investigated QD penetration through the skin. In one of these studies,
163 CdSe/ZnS- mPEG-5000-QDs were injected subcutaneously into CDF1 mice or deposited onto
164 human skin. The results showed that QD diffusion in the dermis is limited by the basement
165 membrane and dense connective tissue fibers; this resulted in negligible QD penetration into
166 the epidermis, hair follicles, sebaceous and sweat glands, nerves, and blood vessels. The total
167 penetration of QDs could only be achieved via a 10-minute massage of damaged or stripped
168 stratum corneum. An increase in pH (8.3) of QD formulations enabled some degree of QD
169 penetration of intact skin [32–34]. Furthermore, simultaneous use of cell therapy and graphene
170 QDs accelerated the repair of skin lesions [35].

171

172 *Brain system*

173 Owing to their nanoscale size, which enables them to cross the blood–brain barrier, QDs
174 represent a revolutionary theranostic tool for the brain system. CdSe/ZnS-streptavidin-QDs
175 injected by stereotaxis into the mouse brain were able to specifically label the microglia in
176 primary cortical cultures via macrophage scavenger receptors and mannose receptors present

177 on their surface, and did not induce toxicity (i.e. induction of inflammation) in the short term
178 [36]. Recently, graphene-QDs were shown to successfully reduce symptoms in mice primed to
179 develop Parkinson's disease by inhibiting fibrillization of α -syn and interacting directly with
180 mature fibrils, thus triggering their disaggregation. These QDs were also to inhibit the
181 aggregation of A β peptides which leads to Alzheimer's disease. These promising results
182 constitute a considerable advance in the treatment of complex pathologies for which no
183 effective therapies are available[37,38].

184

185 *Digestive system*

186 The digestive system is essential for the assimilation of nutrients, immune and endocrine
187 defenses, and the metabolism of endogenous or exogenous molecules (e.g., drugs). A study
188 using CdTe/CdS-QDs administrated by intravenous injection showed that QDs were retained
189 in the sinusoids and selectively taken up by sinusoidal cells (Kupffer cells and liver sinusoidal
190 endothelial cells) within 3 h, but not by hepatocytes[39]. However, the absorption of QDs at
191 the intestinal level has been poorly studied. Previous studies focusing on nanoparticle
192 absorption in general describe the requirement for well-defined characteristics to cross the
193 mucus barrier and the intestinal epithelium lining the intestinal lumen. In nematodes
194 (representative of intestine models), CdTe-QDs influenced lipid metabolism via alteration of
195 the molecular basis of both synthesis and degradation of fatty acid, but not degradation of
196 phospholipids, and increased in fat storage in intestine [40]. The spleens of rats were also
197 exposed by CdSe/CdS-PEG-QDs coupled or not by folic acid with different doses(0–300 nM),
198 and both were revealed to be non-toxic. Moreover, the addition of folic acid significantly
199 improved the uptake of QDs in a dose-dependent manner, highlighting the importance of
200 surface coating properties [41]. VEGFR2-CdSe/ZnS-QDs were used to successfully distinguish
201 between diseased and non-diseased tissue in the colons of carcinogen-treated mice with high

202 sensitivity and specificity. However, the complete removal of the contrast agent by flushing is
203 difficult to achieve [42,43].

204

205 *Pulmonary system*

206 The respiratory system is the preferred site for exchange of gas and airborne particles between
207 the body and the external environment. The evaluation of the efficacy or toxicology of QDs in
208 the pulmonary system is therefore essential. A short-term exposure to 240 µg CdO-QDs/m³ for
209 seven days (3 h/day) caused pulmonary injury and tissue remodeling in mice, and altered
210 immune function [44]. Intratracheal instillation of CdSe/ZnS-QDs or CdSe/ZnS-PEG-QDs
211 persistently induced acute neutrophil infiltration, followed by interstitial lymphocyte
212 infiltration, transiently reduced pulmonary function, and a granulomatous reaction on day 17.
213 Although the granulomatous reaction disappeared for CdSe/ZnS-PEG-QDs at day 90,
214 PEGylation was not sufficient to reduce the risk of side effects associated with QDs [45]. Upon
215 further exploration, genetic predisposition factors and atopy (in this case dust mite allergy) were
216 found to induce impaired pulmonary mechanics by exposure to QDs [46,47].

217

218 *Urinary system*

219 The urinary system is essential for the excretion of endogenous and exogenous substances that
220 are either catabolized or intact. Studies of the kidneys of mice have shown that CdTe-QDs
221 deplete glutathione levels, which reduce the ability of the liver and kidneys to eliminate
222 hydroxyl and superoxide anion radicals, thus inducing oxidative damage to tissues. However,
223 a partial recovery was observed after 28 days [48,49]. Free CdSe/ZnS-QDs and anti-CD47-
224 CdSe/ZnS-QDs were intravesically instilled in mice. Examination of the *in vivo* biodistribution
225 of anti-CD47-CdSe/ZnS-QDs revealed the absence of significant accumulation of QDs outside

226 of the bladder, and no acute toxicity up to 7 days post-administration. Mice showed extravascular
227 biodistribution of QDs under some conditions; however, this was rare [50].

228

229 *Cardiovascular system*

230 The cardiovascular system transports blood from the heart to the peripheral regions of the body
231 and vice versa, and carries a wide variety of substances. The ideal geometry and
232 functionalization capabilities of QDs make them an excellent tool for visualizing the
233 cardiovascular system. Accordingly, CdSe/ZnS-QDs have proved their utility in the study of
234 sarcomere dynamics during excitation-contraction coupling in healthy and diseased cardiac
235 muscle and in the whole heart [51]. By combining *in vivo* cryotechniques and the injection of
236 glutathione-coated QDs into kidneys, QD distribution in the vascular system was achieved,
237 primarily in glomerular blood capillaries for a few seconds and extending to peritubular blood
238 capillaries by five seconds [52]. With regard to therapy, the amorphous form of SeQDs has
239 proved to be effective in prevention of endothelial dysfunction and atherosclerosis [24].

240

241 *Musculoskeletal system*

242 The musculoskeletal system gives form, stability, and movement to the human body. The
243 application of QDs on this system thus far has been confined to imaging. The use of CdSe/ZnS-
244 streptavidin-QDs bound to biotin-phalloidin, which labels skeletal actin filaments, has enabled
245 rapid, quantitative, and inexpensive imaging of sarcomeric movements, notably step-size
246 measurement for low-duty cycle muscle myosin [51,53]. A recent study reported that QDs were
247 mainly found in the synovial membrane, but significantly less on cartilage, one week after being
248 intra-articularly injected into the joints of healthy or osteoarthritis horses [14]. Among the
249 selected articles, no studies were conducted to evaluate the spread of QDs in the bone system,
250 and QD accumulation in bone remains to be defined.

251

252 **Applications of QDs in animals**

253 *Invertebrates*

254 In order to evaluate the integrity of water ecosystems, two aquatic species, polyp *Hydra vulgaris*
255 and coral *Stylophora pistillata*, representative of freshwater and sea habitats, respectively, were
256 exposed to CdSe/ZnS-polymer-QDs and CdTe-QDs at concentrations exceeding the Cd²⁺
257 content in seawater. Despite the presence of a shell and polymer, CdSe/ZnS-polymer-QDs
258 induced dramatic changes, including morphological and global transcriptional changes, albeit
259 less than those induce by CdTe-QDs [54–57]. In order to track the visualization of cyclin E
260 within cells of developing *Xenopus laevis* embryos in real time, CdSe/ZnS-QDs have been
261 coupled to cell-cycle regulatory proteins (recombinant (His6)-cyclin E protein), and their
262 accumulation in the nucleus at midblastula transition (6 h post-fertilization) has been confirmed
263 [58].

264 *Drosophila*, which has high genetic homology with the human genome and has innate immunity
265 signaling pathways that are similar to those of mammals, is an excellent model for
266 genotoxicology and immunotoxicology. QDs were administered via the ingestion of QD-
267 supplemented food (CdSe/ZnS- or InP/ZnS-QDs, 100 and 500 pM) and stress response (hsp70,
268 hsp83), genotoxic stress (p53), and apoptotic cell death (Dredd) genes were observed following
269 the administration of CdSe/ZnS-QDs. However, no significant response was observed
270 following the administration of InP/ZnS-QDs [59].

271

272 *Small vertebrates*

273 Although alternatives to animal studies should be favored, the advantages provided by studies
274 in small animals are not negligible (*i.e.*, transposition of whole biological systems). Various
275 QDs (CdSe/ZnS-QDs, PbS/CdS/ZnS-QDs, CdTe/ZnS-QDs, CdTe-QDs, and QD innovative

276 structures) and modes of administration (intravenous, intraperitoneal, intratracheal, plantar, and
277 oral) were evaluated in mice and rats (Table 3). CdTe-QDs affected steroid hormone and lysine
278 biosyntheses and taurine metabolism [60]. CdSe/ZnS-QDs injected intravenously in mice at a
279 concentration up to 10 mg/kg body weight (BW) did not induce significant toxic effects during
280 four weeks of administration; however, a dose of 20 mg/kg BW caused death in two-thirds of
281 mice shortly after the start of experiment [61]. Biodistribution kinetics of intravenously injected
282 PbS/CdS/ZnS-QDs at 0.04 mg/mL revealed the presence of QDs in the lungs after short time
283 periods (first 0-30 s) followed by accumulation in the liver (60 – 120 s) with complete
284 disappearance of fluorescence at the injection site. After 25 days, elimination by the urinary
285 system lead to the total elimination of the QDs [62,63]. Similarly, biodistribution studies of a
286 single intravenous dose
287 (0.2 $\mu\text{mol/kg}$) of CdTe/ZnS-QDs defined an elimination half-life of 12 - 14 h [64]. After
288 intraperitoneal injection of CdSe/CdS-QDs every 3 days for a period of 15 days, an increase in
289 the levels of LDH, NADPH, and IL-6 pro-inflammatory cytokines was specifically detected in
290 the plasma, liver, and spleen [65]. Globally, QD accumulation in the liver, kidney, and spleen
291 was observed in the four previously cited studies, regardless of route of administration. The
292 injection dose, particle size, and surface charge have been identified as factors affecting mean
293 residence time, apparent volume of distribution, and clearance, particularly in the case of Ag₂S
294 QDs [66]. The assessment of pulmonary toxicity following intratracheal injection of CdSe/ZnS-
295 QDs revealed lung injury and inflammation in a dose-dependent manner, which peaked at days
296 7 and 14 post-exposure, with a holding time of QD fluorescence of 1 week. The built-up of
297 Cd²⁺ occurred only in lung-associated lymph nodes and kidneys for 28 days [67]. An overdose
298 (50 mg/kg) of phospholipid micelle-encapsulated CdSe-CdS/ZnS-PEG-QDs over 112 days (16
299 weeks) did not induce toxicity, despite the accumulation of QDs in the liver and spleen in
300 Kunming mice [68]. The evaluation of orally administered 0.2 mg/kg and 0.4 mg/kg BW/day

301 of CdTe-QDs/quercetin complex for 3 weeks highlighted the utility of QDs as nano-carriers by
302 reducing inflammation significantly and promoting cartilage regeneration [69]. Intraperitoneal
303 injection (10 mg/kg) of graphene QDs effectively ameliorated autoimmune encephalomyelitis
304 [70]. The evaluation of CdSe/ZnS-QDs (10, 20, and 40 mg/kg BW injection) on the male
305 reproductive system at different stages of development was performed in 32 male mice (adult
306 group) and 24 pregnant mice (embryo group) on day 8 of gestation, and no significant effect on
307 fetal testis development and on adult groups at up to 20 mg/kg BW was observed. However, at 40
308 mg/kg BW, a decrease in lamina propria, destruction in interstitial tissue, deformation of
309 seminiferous tubules, and a reduction in number of spermatogonia, spermatocytes, and
310 spermatids was observed [71–73]. Embryotoxicity following the injection of CdTe-QDs on the
311 13th day of gestation in pregnant rats was assessed in 121 fetuses and via histological analysis
312 of placentas. This study revealed dose-dependent survival rates of fetuses (Table 3) due to
313 placental damage rather than QD penetration and accumulation in the fetuses [74], and an
314 impairment on the first two generations of placenta growth [75].

315

316 *Large vertebrates*

317 Biomedical research in large animal models is rare, especially in non-human primates, which
318 are unfortunately irreplaceable as models of certain diseases owing to their close similarity to
319 humans.

320 In the cellular therapy field, assessment of cell migration and adhesion is of paramount
321 importance. CdSe/ZnS-polymer-QDs were used to successfully label and assess the adhesion
322 of goat adipose tissue-derived stem cells (g-ADSCs) after 30, 60, and 90 days of cell infusion
323 in the goat mammary glands. The labeling did not affect cellularity and morphology, and was
324 maintained long-term, even after freezing of liquid NO₂. The health status of goats following
325 QD administration has not been specified. [76].

326 Both phospholipid micelle-encapsulated CdSe/CdS/ZnS-QDs (ph-QDs) [77] and F-127-
327 encapsulated-silicon-QDs [78] were administrated to monkeys (25 and 200 mg/kg BW,
328 respectively) via short intravenous transfusion (30 min). For both QDs, no signs of toxicity
329 were clearly detected in terms of general conditions (body mass, physical, mental, and
330 nutritional behavior), biological parameters (biochemical, no signs of infection or allergic or
331 toxic reactions, liver, and renal). The histological analyses have been unchanged despite QD
332 accumulation in kidney, liver, and spleen, indicating that the breakdown and QDs clearance is
333 quite slow, unlike in mice in which there were signs of delayed and time-dependent increased
334 liver damage (inflammation, proliferation of Kupffer cells, multifocal cholestasis, and spotty
335 necrosis of hepatic cells). The fate of the two types of QDs could not be determined [77,78]. The
336 injection of ph-QDs in pregnant monkeys at a gestational age of 100 days resulted in a
337 miscarriage rate of 60% after having crossed the placenta from the mother to fetus and induced
338 acute hepatocellular injury in the mother after a week of administration [79].

339

340 **Concluding Remarks and Future Perspectives**

341 The rapid expansion of the popularity of QDs has resulted in the publication of a large number
342 of studies on the subject, with high variability in the structure and composition of the QDs
343 studied, thus making synthesis and comparisons difficult (see Outstanding Questions).
344 Nevertheless, 50% of the studies are based on CdSe/ZnS-polymer-QDs produced by the same
345 supplier, which presents both an advantage (comparability of articles) and a limitation (fewer
346 studies on the structure of other semiconductor QDs).

347 At the cellular level, overall toxic effects appear at a certain threshold concentration that differs
348 according to the sensitivity of each cell type [109]. Stem cells appear to be more resistant under
349 certain conditions than differentiated cells, and the presence of QDs does not seem to affect
350 stem cell differentiation. Depending on the intended application (*in vitro* imaging, diagnostic,

351 or theranostic), it is essential to define the optimal concentration range to obtain desired effects
352 and toxicity thresholds for each study, and not conclude, without due investigation, that QDs
353 show global cytotoxicity. Interestingly, the results with innovative QD structures incorporating
354 new materials are encouraging for safer use in medical imaging.

355 With regard to organs, the lungs, kidneys, and the liver are the most affected by toxicity at high
356 concentrations due to QD accumulation. The involvement of these organs is globally observed
357 for all nanoparticles, probably inherent to their size, rather than specifically for QDs [80]. As
358 observed for a number of anticancer and antiretroviral drugs, accumulation in organs might be
359 associated with potential toxicities, but preliminary precautions can be taken (improvement of
360 hydration for nephrotoxic risk, addition of adjuvant protective organ) and does not necessarily
361 constitute an obstacle to their use. Additional studies are needed to adjust QD concentrations
362 according to their use. Surprisingly, the brain seems to be more resistant to the toxic effects of
363 QDs; the same observations have been made at the cellular level, and revolutionary applications
364 in neurodegenerative diseases are being explored.

365 Based on the observed negative effects on the ecosystem, QDs should be used with the same
366 caution as chemotherapy treatments. The studies carried out on small and large animals are
367 encouraging, taking into account the benefit/risk balance; however, animal studies on concrete
368 cases of pathologies have yet to be conducted.

369 Regarding strategies for minimizing toxicity, in the case of stem cells, the addition of a shell
370 reduces toxicity, especially by means of polymerization. Biocompatibility has been achieved
371 by incorporating QDs in glass. For differentiated cells, the addition of a shell associated with
372 polymerization is in some cases not sufficient; the use of QDs in amorphous form or the addition
373 of adjuvant alleviates the effects. Other winning strategies such as functionalization or
374 infiltration into silicone have minimized toxicity. Except for the pulmonary system, where the
375 toxicity can be exacerbated due to factors such as genetic predisposition, the addition of shells

376 associated with polymerization is sufficient to limit the toxicity in the organs. In invertebrates,
377 all cadmium-based QDs, even when combined with a shell, polymerization and
378 functionalization, show toxicity. Only a change to another chemical element in another group
379 reduces the toxicity. For small animals, the preferred means of toxicity minimization is the
380 addition of a multishell. For large vertebrates, all minimization strategies have been
381 successfully applied at once, and these QDs have been proven to be non-toxic, except in the
382 case of pregnancy. Despite their toxicity, semiconductor QDs have been noted for their ability
383 to respond to a wide range of applications. The toxicity of QDs can be exploited favorably to
384 destroy cells that have lost their capacity to die (i.e., tumors) via a controlled toxicology
385 strategy. A strategy of diffusion limitation can also be considered by playing on a galenic
386 formulation without modifying the structure of the QD.

387 Before their potential is fully exploited in biological application, in-depth studies of
388 pharmacokinetics, taking into account all routes of administration, are necessary and must be
389 supplemented by regimens with repeated administrations. The fate of QDs in the body must be
390 further clarified; particularly, the mechanism of elimination must be elucidated.

391 To reach clinical and industrial translation by establishing a pharmaceutical product for human
392 clinical trials, close cooperation between different disciplines (chemist, physicists, biologists,
393 pharmacists, pharmacologists, clinicians) and legal instances is paramount in order to take into
394 account biological and environmental considerations and regulatory requirements (Figure
395 2). For this purpose, it is necessary to agree on a standardized and large-scale QDs preparation
396 method with good and reproducible performance and to define a set of standard quality control
397 for the characterization of QDs. However, between batches, there may always be a lack of
398 reproducibility that should be overcome by additional controls and may be validated by
399 functional tests. Another challenge is to ensure regulations to qualify the raw material in
400 pharmaceutical grade; it is necessary to ensure the absence of heavy metals. However, heavy

401 metals are constituents of semiconductor QDs. Without demonstrating the effectiveness of the
402 toxicity minimization strategies or an argument in favor of controlled toxicology weighing the
403 benefits/risks for certain cases, accompanied by progress in legal regulation, the development
404 of a pharmaceutical preparation that is employable in the clinical setting cannot be envisaged.

405

406 Competing Financial Interests: The authors declare having no conflicts of interest related to this
407 paper.

408

409

410

411 **Box 1. Structure-activity relationship of QDs**

412 A QD is a nanocrystal made of semiconductor materials consisting of a few million atoms (but
413 only a small number of free electrons, ≤ 100) that is small enough to exhibit quantum
414 mechanical properties [81]. QDs can be composed of metallic atoms (e.g. Ni, Co, Pt, Au) or
415 mostly of semiconductor materials, such as elements of periodic group II – VI (CdTe, CdSe,
416 CdS, ZnSe, ZnS, PbS, PbSe, SnTe) [82] or from III – V group such as In and Ga [83]. In addition,
417 QDs can surround by shell often to reduce ion release and therefore, its toxicity [84]. QDs can
418 also be functionalized by adding a terminal function such as - NH₂ or - COOH allowing their
419 hydrophilization [85], polymers to reduce their toxicity or improve their absorption [86],
420 peptides [87] or antibodies [88] to specifically target a biological element (Figure 1).

421

422 **Box 2. Characterization of quantum dots**

423 Initially, their optical properties are evaluated by UV-visible [89] and photoluminescence
424 spectroscopy [90,91], which is a fast and nondestructive technique allowing for the excitation,
425 absorption, and emission spectra used for calculation of quantum yield to be determined [92].
426 The band gap studies were determined by optical diffuse reflectance spectra measurement
427 [93,94]. The size and morphology of QDs can be estimated by scanning or transmission electron
428 microscopy [95], dynamic light scattering (DLS) [96,97], or mathematic approaches from
429 absorption edges using Henglein empirical curve [98]. To define the functionalization, Fourier
430 transformed infrared (FTIR) spectroscopic measurements can be used [99]. The analysis of
431 structure and elemental composition can be performed by X-ray diffraction [83,100] and energy
432 dispersive X-ray analysis [101,102], respectively. Non-destructive techniques such as Raman
433 spectroscopy explore the confined electronic structure of QDs [103–105]. QDs dosage
434 suspension can be achieved by high pressure liquid chromatography via size exclusion
435 chromatography with a fluorimetric detector [106]. The metal ion content in final QDs was also

436 assayed by inductively coupled plasma atomic emission spectrometry [107], and QD behavior
437 was studied by electrochemical methods [108].

438

439

440 **Glossary**

441 **Long-term transepithelial electrical resistance TEER:** commonly used *in vitro* for
442 the assessment of the integrity of the epithelial cell layers.

443

444 **Quantum dots:** The term quantum comes from these mechanical properties at the
445 atomic and subatomic scale with zero-dimensional as a fixed point.

446

447 **Stem cells:** consist of three forms: (i) adult stem cells (ASC) also called stem cells
448 specific to the tissues contained in the body (e.g., hematopoietic, epithelial, neuronal,
449 mesenchymal), (ii) embryonic stem cells or (iii) embryonic germ cells.

450

451 **References**

- 452 1 Himmelstoß, S.F. and Hirsch, T. (2019) A critical comparison of lanthanide based
453 upconversion nanoparticles to fluorescent proteins, semiconductor quantum dots, and carbon
454 dots for use in optical sensing and imaging. *Methods Appl Fluoresc* 7, 022002
- 455 2 Lei, Y. *et al.* (2012) Labeling of hematopoietic stem cells by Tat peptide conjugated quantum
456 dots for cell tracking in mouse body. *J Nanosci Nanotechnol* 12, 6880–6886
- 457 3 Pleskova, S.N. *et al.* (2018) The interaction between human blood neutrophil granulocytes
458 and quantum dots. *Micron* 105, 82–92
- 459 4 Samuel, S.P. *et al.* (2015) CdTe quantum dots induce activation of human platelets:
460 implications for nanoparticle hemocompatibility. *Int J Nanomedicine* 10, 2723–2734
- 461 5 Cepeda-Pérez, E. *et al.* (2016) SERS and integrative imaging upon internalization of
462 quantum dots into human oral epithelial cells. *Journal of Biophotonics* 9, 683–693
- 463 6 Zhao, X. *et al.* (2015) Effect of nonendocytic uptake of nanoparticles on human bronchial
464 epithelial cells. *Anal. Chem.* 87, 3208–3215
- 465 7 Yin, H. *et al.* (2017) Quantum dots modulate intracellular Ca²⁺ level in lung epithelial cells.
466 *Int J Nanomedicine* 12, 2781–2792
- 467 8 Turdalieva, A. *et al.* (2016) Bioelectric and Morphological Response of Liquid-Covered
468 Human Airway Epithelial Calu-3 Cell Monolayer to Periodic Deposition of Colloidal 3-
469 Mercaptopropionic-Acid Coated CdSe-CdS/ZnS Core-Multishell Quantum Dots. *PLoS ONE*
470 11, e0149915
- 471 9 Ando, M. *et al.* (2016) Cytotoxicity of CdSe-based quantum dots incorporated in glass
472 nanoparticles evaluated using human keratinocyte HaCaT cells. *Biosci. Biotechnol.*
473 *Biochem.* 80, 210–213
- 474 10 Shang, W. *et al.* (2014) The uptake mechanism and biocompatibility of graphene
475 quantum dots with human neural stem cells. *Nanoscale* 6, 5799–5806
- 476 11 Zhang, J. *et al.* (2011) Labeling primary nerve stem cells with quantum dots. *J Nanosci*
477 *Nanotechnol* 11, 9536–9542
- 478 12 Corazzari, I. *et al.* (2013) Localization of CdSe/ZnS quantum dots in the lysosomal
479 acidic compartment of cultured neurons and its impact on viability: potential role of ion
480 release. *Toxicol In Vitro* 27, 752–759
- 481 13 Kundrotas, G. *et al.* (2019) Uptake and distribution of carboxylated quantum dots in
482 human mesenchymal stem cells: cell growing density matters. *J Nanobiotechnology* 17, 39

- 483 14 Grady, S.T. *et al.* (2019) Persistence of fluorescent nanoparticle-labelled bone marrow
484 mesenchymal stem cells in vitro and after intra-articular injection. *J Tissue Eng Regen Med*
485 13, 191–202
- 486 15 Fujita, H. *et al.* (2010) Identification of Three Distinct Functional Sites of Insulin-
487 mediated GLUT4 Trafficking in Adipocytes Using Quantitative Single Molecule Imaging.
488 *Mol Biol Cell* 21, 2721–2731
- 489 16 Yoshioka, T. *et al.* Fate of bone marrow mesenchymal stem cells following the
490 allogeneic transplantation of cartilaginous aggregates into osteochondral defects of rabbits.
491 *J Tissue Eng Regen M.* 5, 437–443
- 492 17 Wu, Y. *et al.* (2016) Functional quantum dot-siRNA nanoplexes to regulate
493 chondrogenic differentiation of mesenchymal stem cells. *Acta Biomater* 46, 165–176
- 494 18 Filali, S. *et al.* (2018) Live-stream characterization of cadmium-induced cell death using
495 visible CdTe-QDs. *Sci. Rep.* 8, 12614
- 496 19 Hsieh, M.-S. *et al.* (2009) Cytotoxic Effects of CdSe Quantum Dots on Maturation of
497 Mouse Oocytes, Fertilization, and Fetal Development. *Int J Mol Sci* 10, 2122–2135
- 498 20 Peng, L. *et al.* (2015) Metallomics Study of CdSe/ZnS Quantum Dots in HepG2 Cells.
499 *ACS Nano* 9, 10324–10334
- 500 21 Nguyen, K.C. *et al.* (2015) Mitochondrial Toxicity of Cadmium Telluride Quantum Dot
501 Nanoparticles in Mammalian Hepatocytes. *Toxicol. Sci.* 146, 31–42
- 502 22 Song, S.H. *et al.* (2015) Primary hepatocyte imaging by multiphoton luminescent
503 graphene quantum dots. *Chem. Commun.* 51, 8041–8043
- 504 23 Yan, M. *et al.* (2016) Cytotoxicity of CdTe quantum dots in human umbilical vein
505 endothelial cells: the involvement of cellular uptake and induction of pro-apoptotic
506 endoplasmic reticulum stress. *Int J Nanomedicine* 11, 529–542
- 507 24 Zhu, M.-L. *et al.* (2019) Amorphous nano-selenium quantum dots improve endothelial
508 dysfunction in rats and prevent atherosclerosis in mice through Na⁺/H⁺ exchanger 1
509 inhibition. *Vascul. Pharmacol.* DOI: 10.1016/j.vph.2019.01.005
- 510 25 Jiang, X.-Y. *et al.* (2017) Quantum dot interactions and flow effects in angiogenic
511 zebrafish (*Danio rerio*) vessels and human endothelial cells. *Nanomedicine* 13, 999–1010
- 512 26 Paris-Robidas, S. *et al.* (2016) Internalization of targeted quantum dots by brain
513 capillary endothelial cells in vivo. *J. Cereb. Blood Flow Metab.* 36, 731–742
- 514 27 Trabelsi, H. *et al.* (2013) Subacute toxicity of cadmium on hepatocytes and nephrocytes
515 in the rat could be considered as a green biosynthesis of nanoparticles. *Int J Nanomedicine*
516 8, 1121–1128

517 28 Pujalte, I. *et al.* (2015) Cytotoxic effects and cellular oxidative mechanisms of metallic
518 nanoparticles on renal tubular cells: impact of particle solubility. *Toxicol Res* 4, 409–422

519 29 Yuan, R. *et al.* (2018) Quantum dot-based fluorescent probes for targeted imaging of
520 the EJ human bladder urothelial cancer cell line. *Exp Ther Med* 16, 4779–4783

521 30 Li, Y. *et al.* (2017) Detection of Echinococcus granulosus antigen by a quantum
522 dot/porous silicon optical biosensor. *Biomed Opt Express* 8, 3458–3469

523 31 Courtney, C.M. *et al.* (2016) Photoexcited quantum dots for killing multidrug-resistant
524 bacteria. *Nat. Mater* 15, 529–534

525 32 Kulvietis, V. *et al.* Distribution of polyethylene glycol coated quantum dots in mice
526 skin. *Exp Dermatol.* 22, 157–159

527 33 Prow, T.W. *et al.* (2012) Quantum dot penetration into viable human skin.
528 *Nanotoxicology* 6, 173–185

529 34 Gratieri, T. *et al.* (2010) Penetration of quantum dot particles through human skin. *J*
530 *Biomed Nanotechnol* 6, 586–595

531 35 Haghshenas, M. *et al.* (2019) Use of embryonic fibroblasts associated with graphene
532 quantum dots for burn wound healing in Wistar rats. *In Vitro Cell. Dev. Biol. Anim.* 55, 312–
533 322

534 36 Minami, S.S. *et al.* (2012) Selective targeting of microglia by quantum dots. *J*
535 *Neuroinflammation* 9, 22

536 37 Liu, Y. *et al.* (2015) Graphene quantum dots for the inhibition of β amyloid aggregation.
537 *Nanoscale* 7, 19060–19065

538 38 Kim, D. *et al.* (2018) Graphene quantum dots prevent α -synucleinopathy in Parkinson's
539 disease. *Nat. Nanotechnol.* 13, 812–818

540 39 Liang, X. *et al.* (2015) Intravital Multiphoton Imaging of the Selective Uptake of Water-
541 Dispersible Quantum Dots into Sinusoidal Liver Cells. *Small* 11, 1711–1720

542 40 Wu, Q. *et al.* (2016) Quantum dots increased fat storage in intestine of *Caenorhabditis*
543 *elegans* by influencing molecular basis for fatty acid metabolism. *Nanomed-nanotechnol.*
544 12, 1175–1184

545 41 Haque, M.M. *et al.* (2013) Effects of folic acid and polyethylene glycol coated quantum
546 dots on toxicity and tissue uptake to precision-cut spleen slices of rats. *J Pharm Investig* 43,
547 375–383

548 42 Carbary-Ganz, J.L. *et al.* (2015) In vivo molecular imaging of colorectal cancer using
549 quantum dots targeted to vascular endothelial growth factor receptor 2 and optical coherence
550 tomography/laser-induced fluorescence dual-modality imaging. *J Biomed Opt* 20, 096015

551 43 Carbary-Ganz, J.L. *et al.* (2014) Quantum dots targeted to vascular endothelial growth
552 factor receptor 2 as a contrast agent for the detection of colorectal cancer. *J Biomed Opt* 19,
553 086003

554 44 Blum, J.L. *et al.* (2014) Short-term inhalation of cadmium oxide nanoparticles alters
555 pulmonary dynamics associated with lung injury, inflammation, and repair in a mouse
556 model. *Inhal Toxicol* 26, 48–58

557 45 Wu, T. and Tang, M. (2014) Toxicity of quantum dots on respiratory system. *Inhal*
558 *Toxicol* 26, 128–139

559 46 Scoville, D.K. *et al.* (2018) Quantum dot induced acute changes in lung mechanics are
560 mouse strain dependent. *Inhal Toxicol* 30, 397–403

561 47 Scoville, D.K. *et al.* (2019) Quantum dots and mouse strain influence house dust mite-
562 induced allergic airway disease. *Toxicol. Appl. Pharmacol.* 368, 55–62

563 48 Wang, J. *et al.* (2017) Dose and time effect of CdTe quantum dots on antioxidant
564 capacities of the liver and kidneys in mice. *Int J Nanomedicine* 12, 6425–6435

565 49 Zhao, L. *et al.* (2019) Kidney Toxicity and Response of Selenium Containing Protein-
566 glutathione Peroxidase (Gpx3) to CdTe QDs on Different Levels. *Toxicol. Sci.* 168, 201–208

567 50 Pan, Y. *et al.* (2017) In vivo biodistribution and toxicity of intravesical administration
568 of quantum dots for optical molecular imaging of bladder cancer. *Sci Rep* 7,

569 51 Kobirumaki-Shimozawa, F. *et al.* (2012) Sarcomere Imaging by Quantum Dots for the
570 Study of Cardiac Muscle Physiology. *J Biomed Biotechnol* 2012,

571 52 Terada, N. *et al.* (2016) Application of “In Vivo Cryotechnique” to Visualization of
572 Microvascular Blood Flow in Mouse Kidney by Quantum Dot Injection. In *In Vivo*
573 *Cryotechnique in Biomedical Research and Application for Bioimaging of Living Animal*
574 *Organs* pp. 219–221, Springer, Tokyo

575 53 Wang, Y. *et al.* (2013) The Qdot-labeled actin super-resolution motility assay measures
576 low-duty cycle muscle myosin step size. *Biochemistry* 52, 1611–1621

577 54 Ambrosone, A. *et al.* (2017) Dissecting common and divergent molecular pathways
578 elicited by CdSe/ZnS quantum dots in freshwater and marine sentinel invertebrates.
579 *Nanotoxicology* 11, 289–303

580 55 Liu, T. *et al.* (2014) Hematopoiesis toxicity induced by CdTe quantum dots determined
581 in an invertebrate model organism. *Biomaterials* 35, 2942–2951

582 56 Yan, S.-Q. *et al.* (2016) Reproductive toxicity and gender differences induced by
583 cadmium telluride quantum dots in an invertebrate model organism. *Sci Rep* 6, 34182

584 57 Xing, R. *et al.* (2016) Targeting and retention enhancement of quantum dots decorated
585 with amino acids in an invertebrate model organism. *Sci Rep* 6, 19802

586 58 Brandt, Y.I. *et al.* (2015) Quantum dot assisted tracking of the intracellular protein
587 Cyclin E in *Xenopus laevis* embryos. *J Nanobiotechnol* 13, 31

588 59 Alaraby, M. *et al.* (2015) Assessing potential harmful effects of CdSe quantum dots by
589 using *Drosophila melanogaster* as in vivo model. *Sci. Total Environ.* 530–531, 66–75

590 60 Khoshkam, M. *et al.* (2018) Synthesis, characterization and in vivo evaluation of
591 cadmium telluride quantum dots toxicity in mice by toxicometabolomics approach. *Toxicol.*
592 *Mech. Methods* 28, 539-546

593 61 Bozrova, S.V. *et al.* (2017) Semiconductor quantum dot toxicity in a mouse in vivo
594 model. *J. Phys.: Conf. Ser.* 784, 012013

595 62 Benayas, A. *et al.* (2015) PbS/CdS/ZnS Quantum Dots: A Multifunctional Platform for
596 In Vivo Near-Infrared Low-Dose Fluorescence Imaging. *Adv. Funct. Mater.* 25, 6650–6659

597 63 Yaghini, E. *et al.* (2018) In vivo biodistribution and toxicology studies of cadmium-free
598 indium-based quantum dot nanoparticles in a rat model. *Nanomedicine* 14,2644-2655

599 64 Liu, N. *et al.* (2013) Degradation of aqueous synthesized CdTe/ZnS quantum dots in
600 mice: differential blood kinetics and biodistribution of cadmium and tellurium. *Part Fibre*
601 *Toxicol* 10, 37

602 65 Haque, M.M. *et al.* (2013) Acute toxicity and tissue distribution of CdSe/CdS-MPA
603 quantum dots after repeated intraperitoneal injection to mice. *J Appl Toxicol* 33, 940–950

604 66 Javidi, J. *et al.* (2019) Pharmacokinetics, Tissue Distribution and Excretion of Ag₂S
605 Quantum Dots in Mice and Rats: the Effects of Injection Dose, Particle Size and Surface
606 Charge. *Pharm. Res.* 36, 46

607 67 Roberts, J.R. *et al.* (2013) Lung toxicity and biodistribution of Cd/Se-ZnS quantum dots
608 with different surface functional groups after pulmonary exposure in rats. *Part Fibre Toxicol*
609 10, 5

610 68 Liu, J. *et al.* (2013) Toxicity assessment of phospholipid micelle-encapsulated
611 cadmium-based quantum dots using Kunming mice. *RSC Adv.* 3, 1768–1773

612 69 Jeyadevi, R. *et al.* (2013) Enhancement of anti arthritic effect of quercetin using
613 thioglycolic acid-capped cadmium telluride quantum dots as nanocarrier in adjuvant induced
614 arthritic Wistar rats. *Colloids Surf B Biointerfaces* 112, 255–263

615 70 Tomic, J. *et al.* (2019) Graphene quantum dots inhibit T cell-mediated
616 neuroinflammation in rats. *Neuropharmacology* 146, 95–108

617 71 Amiri, G. *et al.* (2016) Comparison of Toxicity of CdSe: ZnS Quantum Dots on Male
618 Reproductive System in Different Stages of Development in Mice. *Int J Fertil Steril* 9, 512–
619 520

620 72 Xu, G. *et al.* (2016) The Reproductive Toxicity of CdSe/ZnS Quantum Dots on the in
621 vivo Ovarian Function and in vitro Fertilization. *Sci Rep* 6, 37677

622 73 Valipoor, A. *et al.* (2015) A comparative study about toxicity of CdSe quantum dots on
623 reproductive system development of mice and controlling this toxicity by ZnS coverage.
624 *Nanomedicine Journal* 2, 261–268

625 74 Zalgeviciene, V. *et al.* (2017) Quantum dots mediated embryotoxicity via placental
626 damage. *Reprod Toxicol* 73, 222–231

627 75 Hong, W. *et al.* (2019) CdSe/ZnS Quantum Dots Impaired the First Two Generations of
628 Placenta Growth in an Animal Model, Based on the Shh Signaling Pathway. *Nanomaterials*
629 (*Basel*) 9,

630 76 Costa, C.R.M. *et al.* (2017) Labeling of adipose-derived stem cells with quantum dots
631 provides stable and long-term fluorescent signal for ex vivo cell tracking. *In Vitro*
632 *Cell.Dev.Biol.-Animal* 53, 363–370

633 77 Ye, L. *et al.* (2012) A pilot study in non-human primates shows no adverse response to
634 intravenous injection of quantum dots. *Nat. Nanotechnol.* 7, 453–458

635 78 Liu, J. *et al.* (2013) Assessing clinical prospects of silicon quantum dots: studies in mice
636 and monkeys. *ACS Nano* 7, 7303–7310

637 79 Ye, L. *et al.* (2019) Comparing Semiconductor Nanocrystal Toxicity in Pregnant Mice
638 and Non-Human Primates. *Nanotheranostics* 3, 54–65

639 80 Zhang, Y.-N. *et al.* (2016) Nanoparticle–liver interactions: Cellular uptake and
640 hepatobiliary elimination. *J Control Release* 240, 332–348

641 81 Sain, S. *et al.* (2014) Microstructure and photoluminescence properties of ternary
642 Cd_{0.2}Zn_{0.8}S quantum dots synthesized by mechanical alloying. *J Nanopart Res* 16, 2673

643 82 Azpiroz, J.M. *et al.* (2014) Benchmark Assessment of Density Functional Methods on
644 Group II-VI MX (M = Zn, Cd; X = S, Se, Te) Quantum Dots. *J Chem Theory Comput* 10,
645 76–89

646 83 Daly, A.B. *et al.* (2017) Optical and structural properties in type-II InAlAs/AlGaAs
647 quantum dots observed by photoluminescence, X-ray diffraction and transmission electron
648 microscopy. *Superlattices Microstruct.* 110, 1–9

649 84 Abbasi, S. *et al.* (2017) CdSe and CdSe/CdS core-shell QDs: New approach for
650 synthesis, investigating optical properties and application in pollutant degradation.
651 *Luminescence* 32, 1137–1144

652 85 Spirin, M.G. *et al.* (2013) Hydrophilization of CdSe quantum dots with surfactants.
653 *Colloid J* 75, 427–432

654 86 Bobrovsky, A. *et al.* (2016) Quantum dot–polymer composites based on nanoporous
655 polypropylene films with different draw ratios. *Eur Polym J* 82, 93–101

656 87 Thovhogi, N. *et al.* 27-Apr-(2018) Peptide-functionalized quantum dots for potential
657 applications in the imaging and treatment of obesity. *Int J Nanomedicine* 13, 2551-2559

658 88 Brazhnik, K. *et al.* (2014) Advanced Procedure for Oriented Conjugation of Full-Size
659 Antibodies with Quantum Dots. In *Quantum Dots: Applications in Biology* pp. 55–66,
660 Humana Press, New York, NY

661 89 Mansur, H.S. and Mansur, A.A.P. (2011) CdSe quantum dots stabilized by carboxylic-
662 functionalized PVA: Synthesis and UV–vis spectroscopy characterization. *Mater Chem Phys*
663 125, 709–717

664 90 Alemu, Y.A. *et al.* (2018) Enhanced photoluminescence from CuInS₂/ZnS quantum
665 dots: Organic superacid passivation. *Mater. Lett.* 219, 178–181

666 91 Ahia, C.C. *et al.* (2018) Photoluminescence and structural properties of unintentional
667 single and double InGaSb/GaSb quantum wells grown by MOVPE. *Physica B: Condensed*
668 *Matter* 535, 13–19

669 92 Grabolle, M. *et al.* (2009) Determination of the Fluorescence Quantum Yield of
670 Quantum Dots: Suitable Procedures and Achievable Uncertainties. *Anal. Chem.* 81, 6285–
671 6294

672 93 Borah, P. *et al.* (2018) Quantum confinement induced shift in energy band edges and
673 band gap of a spherical quantum dot. *Physica B: Condensed Matter* 530, 208–214

674 94 Marotti, R.E. *et al.* (2006) Crystallite size dependence of band gap energy for
675 electrodeposited ZnO grown at different temperatures. *Sol. Energy Mater Sol.* 90, 2356–
676 2361

677 95 Sinclair, R. *et al.* (2014) The Stanford Nanocharacterization Laboratory (SNL) and
678 Recent Applications of an Aberration-Corrected Environmental Transmission Electron
679 Microscope. *Adv Eng Mater* 16, 476–481

680 96 Ramírez-García, G. *et al.* (2015) Functionalization and characterization of persistent
681 luminescence nanoparticles by dynamic light scattering, laser Doppler and capillary
682 electrophoresis. *Colloids Surf B Biointerfaces* 136, 272–281

683 97 Ramírez-García, G. *et al.* (2017) Characterization of phthalocyanine functionalized
684 quantum dots by dynamic light scattering, laser Doppler, and capillary electrophoresis. *Anal*
685 *Bioanal Chem* 409, 1707–1715

686 98 Henglein, A. (1989) Small-particle research: physicochemical properties of extremely
687 small colloidal metal and semiconductor particles. *Chem. Rev.* 89, 1861–1873

688 99 Shim, M. *et al.* (2000) Long-Lived Delocalized Electron States in Quantum Dots: A
689 Step-Scan Fourier Transform Infrared Study. *J. Phys. Chem. B* 104, 1494–1496

690 100 Bonu, V. and Das, A. (2013) Size Distribution of SnO₂
691 Quantum Dots Studied by UV–Visible, Transmission Electron Microscopy and X-Ray
692 Diffraction. *Mapan* 28, 259–262

693 101 Choi, Y.J. *et al.* (2012) Cyto-/genotoxic effect of CdSe/ZnS quantum dots in human
694 lung adenocarcinoma cells for potential photodynamic UV therapy applications. *J Nanosci*
695 *Nanotechnol* 12, 2160–2168

696 102 Takahashi, C. *et al.* (2017) Imaging of intracellular behavior of polymeric nanoparticles
697 in *Staphylococcus epidermidis* biofilms by slit-scanning confocal Raman microscopy and
698 scanning electron microscopy with energy-dispersive X-ray spectroscopy. *Mater Sci Eng C*
699 76, 1066–1074

700 103 Cepeda-Pérez, E. *et al.* (2016) Interaction of TGA@CdTe Quantum Dots with an
701 Extracellular Matrix of *Haematococcus pluvialis* Microalgae Detected Using Surface-
702 Enhanced Raman Spectroscopy (SERS). *Appl Spectrosc* 70, 1561–1572

703 104 Kostić, R. *et al.* (2017) Off-Resonant Raman Spectroscopy of ZnS Quantum Dots. In
704 *Proceedings of the IV Advanced Ceramics and Applications Conference* pp. 203–215,
705 Atlantis Press, Paris

706 105 Biermann, A. *et al.* (2017) Interface formation during silica encapsulation of colloidal
707 CdSe/CdS quantum dots observed by in situ Raman spectroscopy. *J Chem Phys* 146, 134708

708 106 Pitkänen, L. and Striegel, A.M. (2016) Size-exclusion chromatography of metal
709 nanoparticles and quantum dots. *Trends Analyt Chem* 80, 311–320

710 107 Hao, C.L. (2012), In Vivo Stability and Biodistribution of Quantum Dots by Inductively
711 Coupled Plasma-Atomic Emission Spectrometry. , in *Advanced Materials Research*, 412,
712 pp. 449–452

713 108 Gondim, C.S. *et al.* (2018) Development and Validation of an Electrochemical
714 Screening Methodology for Sulfonamide Residue Control in Milk Samples Using a
715 Graphene Quantum Dots@Nafion Modified Glassy Carbon Electrode. *Food Anal. Methods*
716 11, 1711–1721

717 109 Bilal, M. et al. (2019) Bayesian Network Resource for Meta-Analysis: Cellular
718 Toxicity of Quantum Dots. Small , 1900510.
719
720
721

722 Figure legends

723

724 Figure 1: Schematic illustration of the structure-activity relationship of QDs. Since the
725 inorganic core is biologically inactive, a hydrophilization step is necessary for its use in
726 biological applications. In order to minimize core-induced toxicity, surface modification
727 strategies may be envisaged (i.e., a capping, a polymerization and a functionalization).

728

729 Figure 2: Impact of QDs toxicity including biological and environmental considerations and
730 reglementary requirements for QD use in human.

731

732

733 Table 1: Biological effects depending on the structure of QDs and the type of stem cells or differentiated cells.

Core material	Shell material	Functionalization/Encapsulation	Type of cell	Outcome	Reference	
<i>Stem cells</i>						
CdTe-QDs	-	-	Epithelial	Toxicity	[6]	
	-	-	Synoviocytes	Monitoring, toxicity	[18]	
CdSe-QDs	-	-	Embryonic	Concentration dependent toxicity	[19]	
	ZnS	-	Epithelial	Toxicity	[6]	
		-	Embryonic	↘ toxicity	[19]	
		-	Neuronal	Slight toxicity	[11]	
	-	Anti-myc antibody	Adipocytes	Monitoring	[15]	
	-	Anti-mortalin antibody	Chondrocytes	Monitoring	[16]	
	-	Tat Peptide	Hematopoietic	Monitoring	[2]	
	-	CdS/ZnS	-	Epithelial	± toxicity	[7,8]
	-	ZnS - polymer	-	Embryonic	↘ toxicity	[19]
	-	-	-	Neuronal	No toxicity under threshold detection	[10,11]
-	-	SiSOX9	Chondrocytes	Monitoring	[17]	
Graphene-QDs	-	-	Epithelial	No toxicity under threshold detection	[9]	
	-	-	Neuronal	No toxicity under threshold detection	[10]	
<i>Differentiated cells</i>						
CdTe-QDs	-	-	Endothelial	Toxicity	[21]	
	-	-	Platelets	Toxicity	[4]	
	-	-	Renal	Toxicity	[28]	
	-	-	Renal	Toxicity	[27]	
CdSe-QDs	ZnS	L-cysteine	Renal	Toxicity	[27]	
		-	Monocytes, neutrophils, granulocytes	Toxicity	[3]	
		-	Lymphocytes	No toxicity under threshold detection	[3]	
	-	Hepatocytes	Toxicity	[20]		
	-	Urothelial	No toxicity under threshold detection	[29]		
	-	Photoexcited	Multidrug-resistant bacteria	Bactericidal	[31]	
	-	Anti-Ri7 antibody	Endothelial	Built-up	[25]	
	-	Anti-p38 antibody infiltrated in porous silicon pores immobilized Egp38 antigen	Parasites	Detection	[30]	
Graphene-QDs	ZnS - PEG	-	Endothelial	Built-up	[24]	
	-	-	Hepatocytes	No toxicity under threshold detection	[22]	

734 Table 2: Biological effects depending on the structure of QDs and the organs.

Core material	Shell material	Functionalization	Type of organ	Outcome	Reference
CdTe-QDs	-	-	kidney	Toxicity	[48,49]
	-	-	Intestine	Toxicity	[40]
CdO-QDs	CdS	-	Liver	Monitoring	[39]
	-	-	Lung	Toxicity	[44]
CdSe-QDs	ZnS	-	Brain	No toxicity under threshold detection, visualization	[36]
		-	Heart	Monitoring	[51]
		-	Bladder	No toxicity under threshold detection, no diffusion	[46]
		-	Lung	Toxicity	[45]
		-	Joint	No toxicity under threshold detection	[14]
		GSH	Vascular	Monitoring	[52]
		VEGFR2	Tumor	Detection	[42,43]
		Biotinylated phalloidin	Muscle	Monitoring	[51,53]
		Anti-CD47 antibody	Bladder	No toxicity under threshold detection, no diffusion	[50]
		ZnS - polymer	-	Skin	No penetration
	Graphene-QDs	-	-	Lung	Toxicity
-			Spleen	No toxicity under threshold detection	[41]
Folic acid			Spleen	Built-up	[41]
-			Skin	Therapy	[35]
-			Brain	Therapy	[37-38]

735

736

737 Table 3: Biological effects depending on the structure of QDs and the animal species.

Core material	Shell material	Functionalization /Encapsulation	Animal species	Outcome	Reference
CdTe-QDs	-	-	Mice	Toxicity	[60]
	-	-	Pregnant rat	Dose-dependent embryotoxicity	[74-75]
	-	Quercetin complex	Rat	Therapy	[69]
CdSe-QDs	ZnS	-	Mice	Half-life = 12 – 14h	[64]
	ZnS or CdS	-	Drosophila	Toxicity	[59]
		-	Mice	Dose-dependent toxicity	[61]
	ZnS - polymer	-	Rat	Toxicity	[65]
		-	Male reproductive system in mice	Dose-dependent toxicity	[71-73]
		(His6)-Cyclin E protein	Aquatic species	Monitoring	[58]
		-	Aquatic species	Toxicity	[54-57]
		-	Goat	Monitoring	[76]
	PbS/ZnS	Phospholipid micelle-encapsulated	Mice	No toxicity under threshold detection	[68]
-		Mice	No toxicity under threshold detection	[62;63]	
Phospholipid micelle-encapsulated		Primate	No toxicity under threshold detection	[77]	
InP-QDs	ZnS	-	Pregnant primate	Toxicity	[79]
		-	Drosophila	No toxicity under threshold detection	[59]
Graphene-QDs	-	-	Rat	Therapy	[70]
Silicon-QDs	- polymer	-	Primate	No toxicity under threshold detection	[78]

738

739

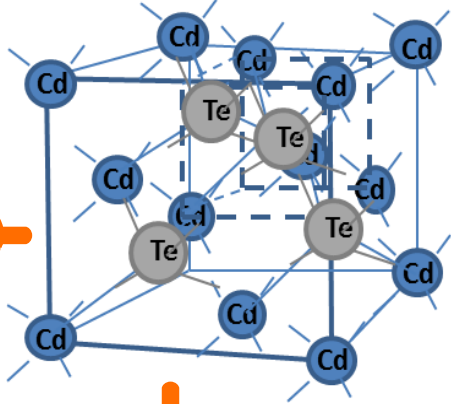
Hydrophilization

↗ water solubility
Biologically compatible



Aqueous coating

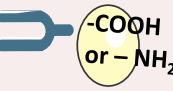
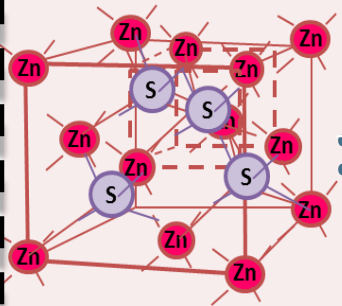
Inorganic core



Organic ligands

Biologically incompatible

Inorganic shell



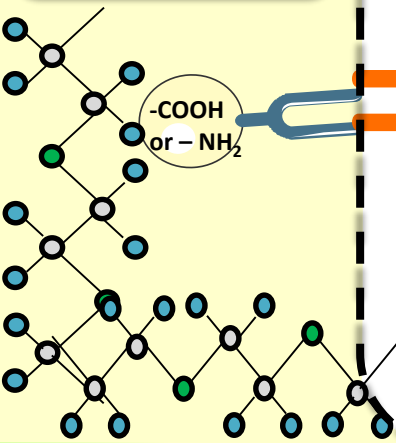
↗ Photostability
↗ Brightness
↘ Photo-oxidation
↗ Solubility
↗ durability of core

Functionalization

Targeted therapy
Biomarker
Detection & Specific diagnosis
Molecular imaging

Polymerization

Biocompatibility
Stability
Amphiphilic
Facilitated conjugation



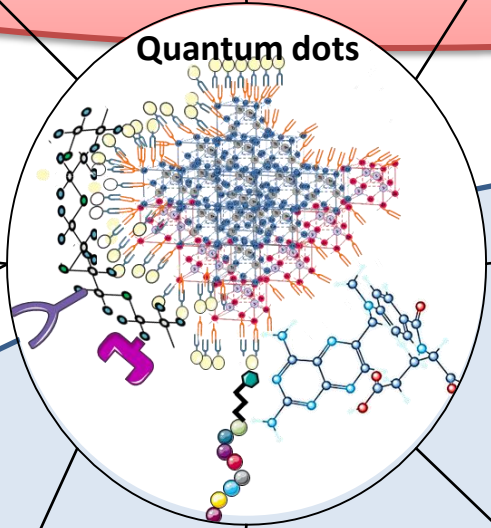
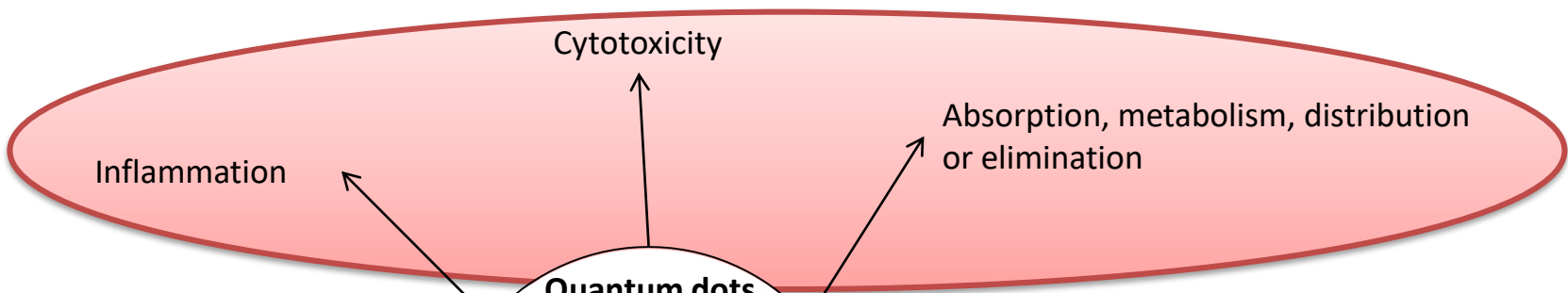
Receptors

Antibody

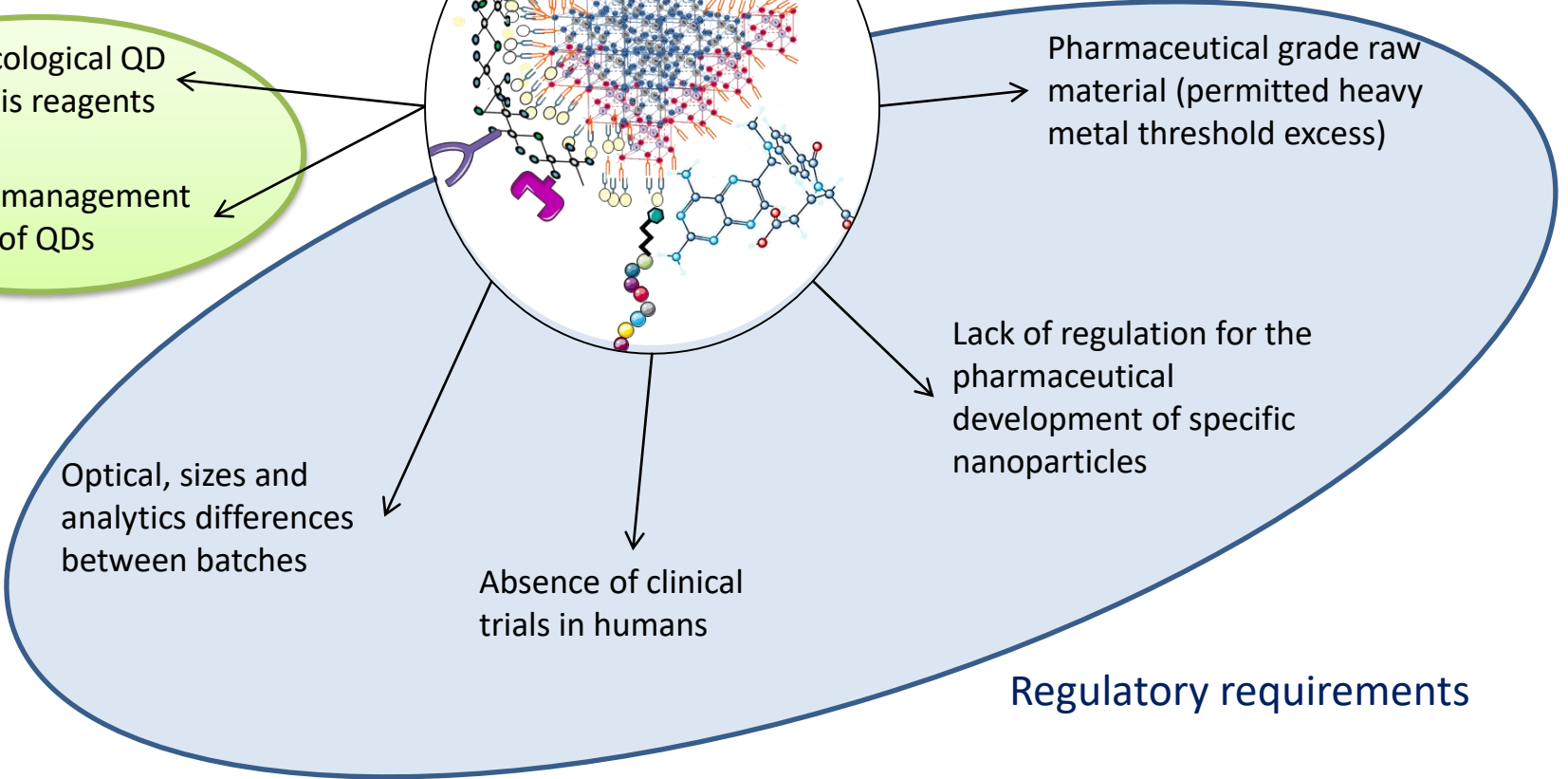
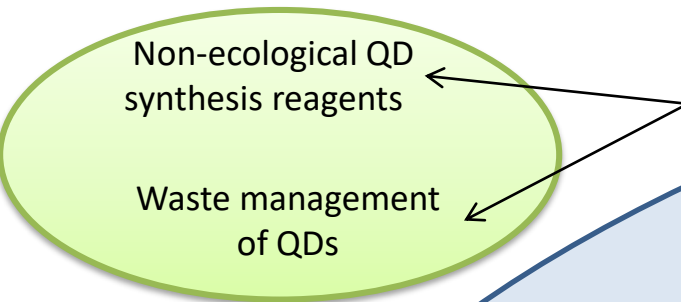
Biotinylated peptides

Drugs

Biological considerations



Environmental considerations



Regulatory requirements